



## Evaluation of the mechanical properties and corrosion behaviour of coconut shell ash reinforced aluminium (6063) alloy composites

Oluyemi Ojo DARAMOLA<sup>1\*</sup>, Adeolu Adesoji ADEDIRAN<sup>1</sup>,  
and Ayodele Tolu FADUMIYE<sup>2</sup>

<sup>1</sup>*Metallurgical and Materials Engineering Department, Federal University of Technology Akure, Ondo State*

<sup>2</sup>*Mechanical Engineering Department, Landmark University, Omu-Aran, Kwara State*

E-mails: [ojaythompson@yahoo.com](mailto:ojaythompson@yahoo.com), [dladesoji@yahoo.com](mailto:dladesoji@yahoo.com)

\* Corresponding author: +2348166814002

### Abstract

Aluminium 6063/Coconut shell ash (CSAp) composites having 3-12 weight percent (wt%) coconut shell ash were fabricated by double stir-casting method. The microstructure, ultimate tensile strength, hardness values, density and corrosion behaviour in 0.3M H<sub>2</sub>SO<sub>4</sub> and 3.5wt% NaCl solution of the composites were evaluated. The density of the composites exhibit a linear and proportional decreased as the percentage of coconut shell ash increases in the aluminium alloy. It implies that composites with lower weight component can be produced by adding CSAp. The microstructural analysis showed uniform distribution of coconut shell ash particles in the aluminium alloy matrix. Significant improvement in hardness and ultimate tensile strength values was noticeable as the wt% of the coconut shell ash increased in the alloy, although this occur at the expense of ductility of the composites as the modulus of elasticity of the composites decreases as the percentage of CSAp increases. Hence, this work has established that incorporation of coconut shell particles in aluminum matrix can lead to the production of low cost aluminum composites with improved hardness and tensile strength values.

### Keywords

Coconut shell; Composite; Matrix; Aluminium 6063; Stir casting; Corrosion; Mechanical properties

## **Introduction**

Aluminium matrix composites (AMCs) are reported to be unique combination composites with mechanical, physical and chemical properties which are scarcely attainable with the use of monolithic materials [1]. In comparison with steel, AMCs stands tall in wide range of engineering applications [2]. Currently, AMCs finds areas of application in the design of components of automobiles, sports and recreation among others [3]. Their choice in automobile and aerospace application is inform by property such as high specific strength and stiffness, low thermal coefficient of expansion, corrosion and high temperature resistance. Madakson et al [4] reported that reinforcement material determines significantly the overall desired property of a developed composite. In an attempt of overcoming the limitations from the high cost of metal matrix composites (MMCs); resulting from interfacial reactions and high density of the most commonly used ceramic reinforcements compared to Aluminium alloys, growing interest of researchers has been drawn to the use of agro waste as secondary reinforcement in composite fabrication [5-7]. The higher deposit of silica and hematite in this agro-waste makes it desirable as reinforcement [3, 8]. However,  $\text{SiO}_2$  is the principal constituent in coconut shell ash [9, 10]. Coconut shell-being an agro-waste is available in large quantity in Nigeria. Traditionally, in some part of Nigeria, it is locally used as fuel for cooking. Also, it serves as a source of fuel, especially for the black smith in their forging process. Alaneme et al. [11] observed the significance of investigating the corrosion behaviour of AMCs. They noted that AMCs interact with acidic environment especially when in marine industries, hence a candidature for investigation. The current work is part of recent effort aimed at considering the potentials of a wide range of agro waste ashes for the development of low cost-high performance aluminium based composites with potentials for use in stress bearing and wears applications among others. The work is motivated by the prospect of developing high performance Aluminium matrix hybrid composites using coconut shell ash particles as reinforcement.

## **Material and method**

The chemical composition of the Aluminium alloy used was determined and the result is presented in Table 1. The Aluminium alloy serves as the matrix for the investigation while processed ash derived from a controlled burning of coconut shell sourced locally were utilized

as reinforcing particulates for the Aluminium matrix.

**Table 1.** Composition of the Aluminium (6063) alloy

Si	Fe	Cu	Mn	Mg	Zn	Cr	Ti	Al
0.45	0.22	0.02	0.03	0.05	0.02	0.03	0.02	balance

***Preparation of coconut shell ash (CSA) and composite production***

The coconut shell was sourced for locally, crushed and burned in a controlled atmosphere with the aid of a perforated metallic drum. The coconut shell was left to burn completely and the ashes removed 24hrs later. The ash was then conditioned by heat-treating at a temperature of 650°C for 180mins to reduce the carbonaceous and volatile constituents of the ash in accordance with [12]. The chemical composition of the CSA was determined and the result is presented in Table 2.

**Table 2.** Chemical composition of the Coconut Shell Ash (CSA)

Al <sub>2</sub> O <sub>3</sub>	CaO	Fe <sub>2</sub> O <sub>3</sub>	K <sub>2</sub> O	MgO	Na <sub>2</sub> O	SiO <sub>2</sub>	MnO	ZnO
15.6	0.57	12.4	0.52	16.2	0.45	45.05	0.22	0.3

Sand casting process was utilized to produce the composites. The process started with the determination of the quantity of Aluminium and CSAP required to produce 3, 6, 9, 12 and 15% weight CSA reinforced composites. CSA particles were initially preheated to remove moisture and to help improve wettability with the Aluminium alloy melt. The alloy ingots were charged into a gas-fired crucible furnace and heated to a temperature of 750±30°C and the liquid alloy was then allowed to cool in the furnace to a semi solid state at a temperature of about 600°C [5, 7]. At this temperature, the preheat CSA particulates were added and stirring of the slurry was performed manually for 5–10 minutes. The composite slurry was then superheated to 720°C and a second stirring performed using a mechanical stirrer for 10 minutes to help improve the distribution of the particulates in the molten Aluminium alloy. The molten composite was then cast into prepared sand moulds. Aluminium (6063) alloy without reinforcement was also prepared for control experimentation.



**Figure 1.** (a) and (b) showing as-cast samples and gas-fired crucible furnace respectively

### **Heat treatment and density measurement**

The cast composites along with the un-reinforced alloy were subjected to cold deformation using a miniature cold rolling machine. The composites was rolled to 20% degrees of deformation using the round orifice of the cold rolling machine before heat treatment was performed by heating the samples at 500°C for 1 hour and quenching in water for each sample.



**Figure 2.** Showing cold rolling process on miniature cold rolling machine

The density measurements were carried out to determine the porosity levels of the composites produced. This was achieved by comparing the experimental and theoretical densities of each weight percent CSA reinforced composite. The weight of the samples was evaluated by weighing the test samples using a high precision weighing balance with a tolerance of 0.1mg. The experimental density was determined by dividing the measured weight of a test sample by its measured volume; while the theoretical density was evaluated using the rule of mixtures given by:

$$\rho_{AA6063/CSAp} = wt._{AA6063} \times \rho_{AA6063} + wt._{CSA} \times \rho_{CSA} \quad (1)$$

where  $\rho_{AA6063/CSAp}$  = density of Composite,  $wt._{AA6063}$  = weight fraction of Aluminium (6063) alloy,  $\rho_{AA6063}$  = density of Aluminium (6063) alloy,  $wt._{CSA}$  = weight fraction CSA, and  $\rho_{CSA}$  = density of CSA.

The percent porosity of the composites was evaluated using the relations [13]:

$$\% \text{ porosity} = (\rho_t - \rho_{ex}) / \rho_t \times 100\% \quad (2)$$

where  $\rho_t$  is the theoretical density ( $\text{g}/\text{cm}^3$ ),  $\rho_{ex}$  is the experimental density ( $\text{g}/\text{cm}^3$ ).

### **Hardness and tensile behaviour**

The hardness of the composites was evaluated using an Indenter micro-hardness Tester. Prior to testing, test specimens cut out from each composite composition were polished to obtain a flat and smooth surface finish. A load of 100g was applied on the



specimens and the hardness profile was evaluated following standard procedures. Multiple hardness tests were performed on each sample and the average value taken as a measure of the hardness of the specimen. The tensile properties of the samples were evaluated by conducting tension test on round tensile samples machined from the composites with dimensions of 5mm diameter and 40 mm gauge length. The tensile test was performed at room temperature (25°C) using a Instron universal testing machine operated at a constant cross head speed of 1mm/s. The machined specimen dimensions and test procedures were in accordance with the specifications of ASTM E8M [14]. Three repeated tests were performed for each composite composition to assess reproducibility of results and hence guarantee reliability of the data generated. The tensile properties evaluated from the tensile test are: the ultimate tensile strength ( $\sigma_u$ ), and the strain to fracture ( $\epsilon_f$ ).

### ***Corrosion test***

The corrosion behaviour of the composites was studied by weight loss method using mass loss and corrosion rate measurements as basis for evaluating the results generated. The corrosion test was carried out by immersion of the test specimens in 0.3M H<sub>2</sub>SO<sub>4</sub> and 3.5wt% NaCl solutions which were prepared following standard procedures. The specimens for the test were cut and then mechanically polished with emery papers from 220 down to 600 grits to produce a smooth surface. The samples were de-greased with acetone, rinsed in distilled water, and then dried in air before immersion in still solutions of 0.3M H<sub>2</sub>SO<sub>4</sub> and 3.5wt% NaCl at room temperature (25°C). The corrosion setups were exposed to atmospheric air for the duration of the immersion test. The weight loss readings were monitored on three day intervals for a period of 18days. Mass loss (mg/cm<sup>2</sup>) for each sample was evaluated in accordance with ASTM G31 standard recommended practice [15] following the relation:

$$m.l = CW/A \quad (3)$$

where m.l is the mass loss (mg/cm<sup>2</sup>), CW is the cumulative weight loss (mg), and A is the total surface area (T.S.A) of the sample (cm<sup>2</sup>). Corrosion rate for each sample was evaluated from the weight loss measurements following the relation [15];

$$C.R = KW/(\rho At) \quad (4)$$

where C.R is corrosion rate (mmy), W is weight loss (g),  $\rho$  is the density (g/cm<sup>3</sup>), A is the area (cm<sup>2</sup>), t is time (hours), and K is a constant equal to 87500.

$$W = W_i - W_f \quad (5)$$

where W is the weight loss (g),  $W_i$  is the initial weight (g) and  $W_f$  is the final weight (g).

## Results and discussion

### *Microstructural examination*

A representative metallurgical microscopic examination showing the morphology of the surface profiles of the CSA reinforced Aluminium composites produced is represented by Figure.3; shows the optical photomicrographs of the Al6063/3%CSA composite.

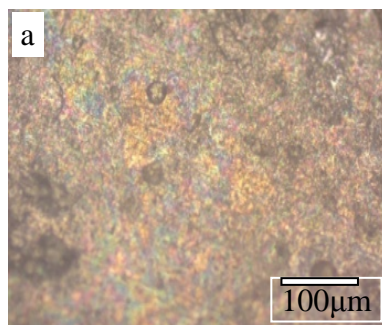


**Figure 3.** Photomicrograph of AA6063/3% wt CSA composite particles dispersed in the AA6063 matrix.

From Figure 3 above, it was observed that the reinforcing particles (CSAp) are visible and clearly delineated in the microstructure and the particles are fairly well distributed in the Aluminium matrix and signs of particle clusters are minimal.

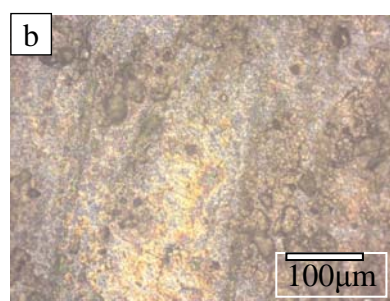


**Figure 4.** Photomicrograph of AA6063/ control sample

Figure 4 is a representative micrograph of the control sample AA6063- being the matrix, showing the spatial arrangement of silicon, iron and aluminium in the microstructure.

### *Composite density and estimated percentage porosity*

The combination of equations 1 and 2 was used in determining the percent porosity

**Table 3.** Composite density and estimated percent porosity

Sample (%CSA)	Mass	Exp. density	Theo. density	Porosity %
A (3)	66.63	2.650	2.681	1.116
B (6)	66.17	2.632	2.661	1.104
C (9)	65.73	2.614	2.642	0.965
D (12)	65.12	2.590	2.622	1.126

From table 3, the experimental densities were discovered to be lower than the theoretical densities owing to the vicinity of porosities in all the composites.

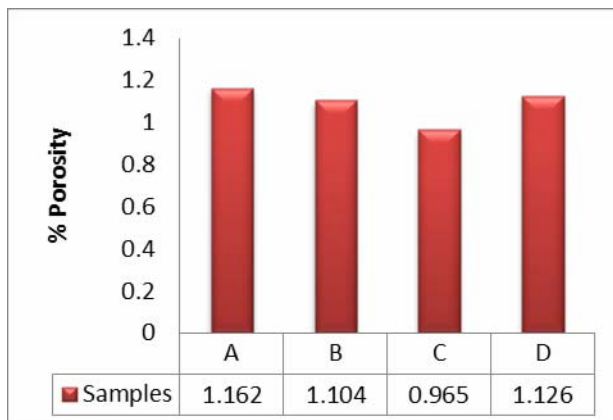


**Figure 5.** Shows the variation of the % porosity for AA6066-CSA composite

A representative of percent porosity for AA6063-CSA composites is illustrated in Figure 5 above. It is apparent by comparison, that the theoretical and experimental densities of the composites exhibit slight porosities difference in the composites. The use of CSA as reinforcements results in the decrease in density of the composites and did not lead to any significant rise in porosity level of the composites when compared to the as received samples

### **Mechanical properties**

The Variation of hardness and ultimate tensile strength are presented in Figures 6 and 7.

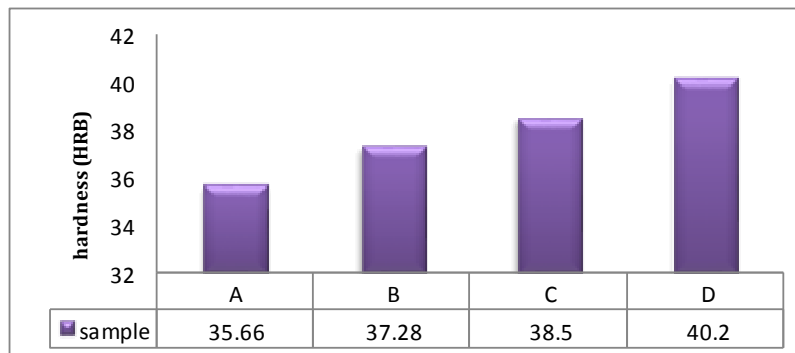


**Figure 6.** Shows the variation of hardness with mass fraction of CSA in reinforced AA6063/CSA composite

The chart trend represented in Figure 6 above shows a significant yield in the hardness value as a result of varying the proportion of CSA.

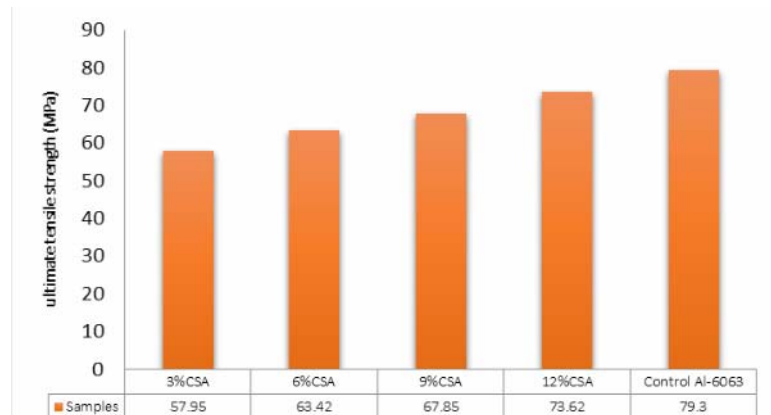


**Figure 7.** Shows the variation of UTS for the single and hybrid reinforced AA6063/CSA composite

The figures above show clearly that the hardness and ultimate tensile strength of the composites observed to increase with the addition of coconut shell ash (CSA) in tandem with [16]. The cold rolling and heat treatment helped in achieving a refined and homogenous structure by removing voids and micro-voids and also aided in redistributing the particulates and second phase particles resulting in considerable elimination of particle clusters and segregation. The elimination of a considerable amount of defects in the composite during cold rolling helped in enhancing the strain hardening capacity of the composite. It was observed that the hardness of the composites increases with an increase in coconut shell ash (CSA). This might have been due to the stoichiometry ratio of  $\text{SiO}_2$  to  $\text{Al}_2\text{O}_3$ , the latter was reported by [17].

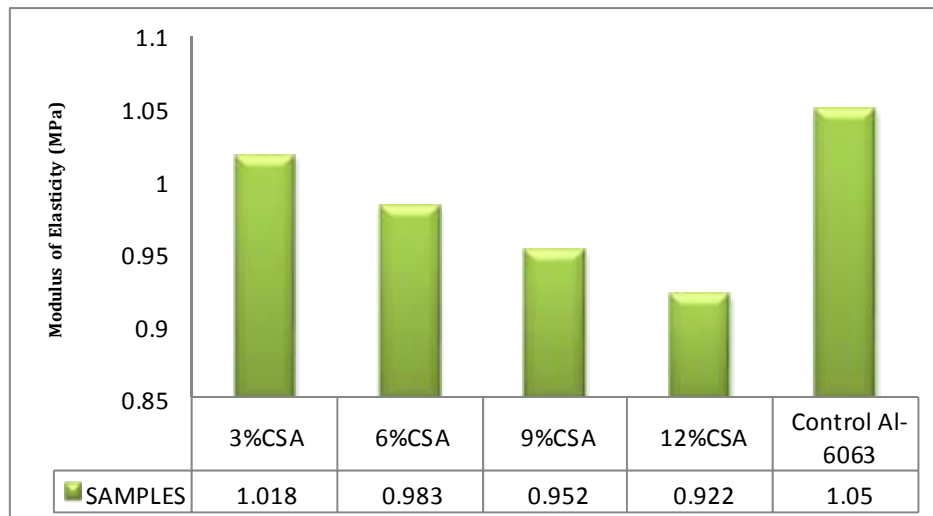


**Figure 8.** Shows the variation of Modulus of Elasticity for the control sample and reinforced AA6063/CSA composite

In Figure 8 however, the modulus of elasticity at 12% CSA witness 12% reduction in comparison to other composites in the series. The more the % CSA added to the composite, the lesser the modulus of elasticity. However, the % wt CSA significantly influences the modulus of elasticity at 3%CSA. The elastic modulus decreased as the percentage of coconut shell ash particles increases in the alloy. This is an index that the incorporation of coconut shell ash particles in the Aluminium matrix reduces the ductility of the material.

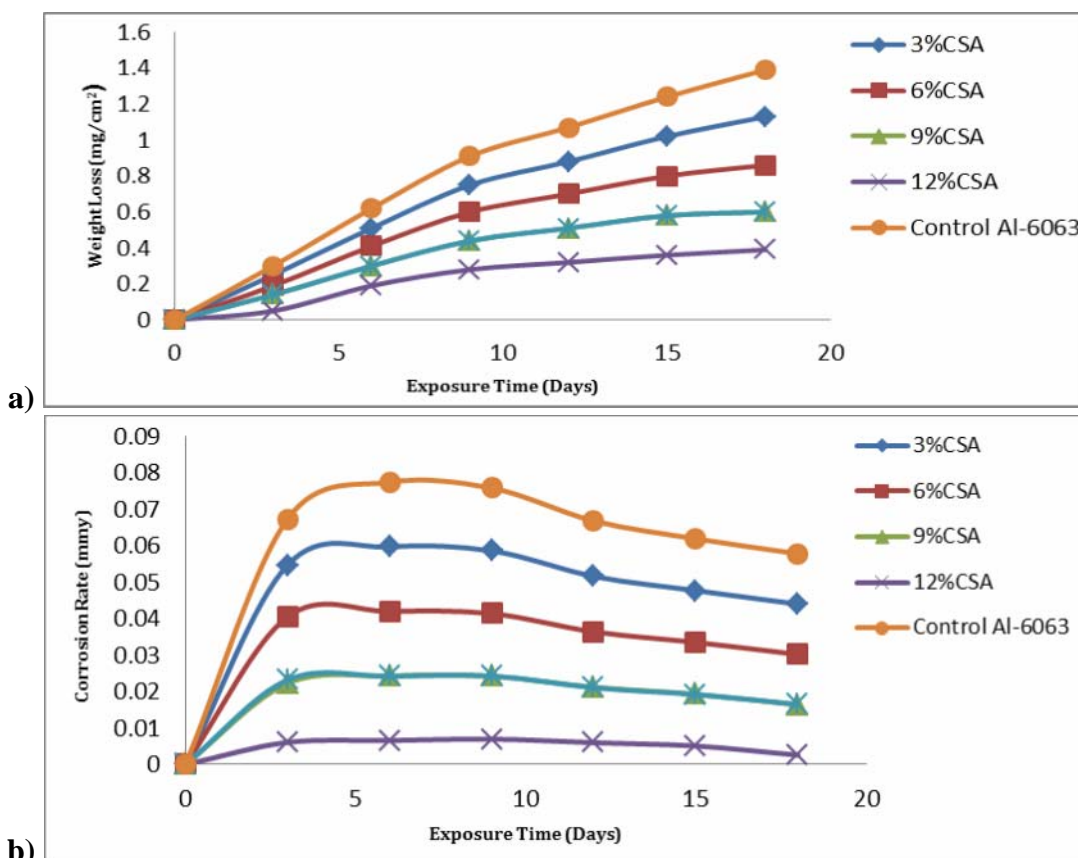


**Figure 9(a) and (b).** Variation of (a) weight loss and (b) corrosion rate with exposure time for a CSA reinforced composites in 0.3 M  $H_2SO_4$  solution

Figure 9 (a) and (b) are representative plots of variations of weight loss and corrosion rate with exposure time for the composites immersed in 0.3 M  $H_2SO_4$  solution. From fig.9a, it was observed that the weight loss increases with increase in exposure time. This might be attributed to the passive film formed on the composites which was unable to give adequate protection to the substrates, hence, the addition of CSAp promoted corrosion resistance of the composites. Furthermore it was observed that among the composites, the weight loss is more pronounced in sample A which is composed of 3wt%CSAp as the reinforcement. This suggest

that the composite containing lower percentage of CSA may not be suitable for use in acidic environments.

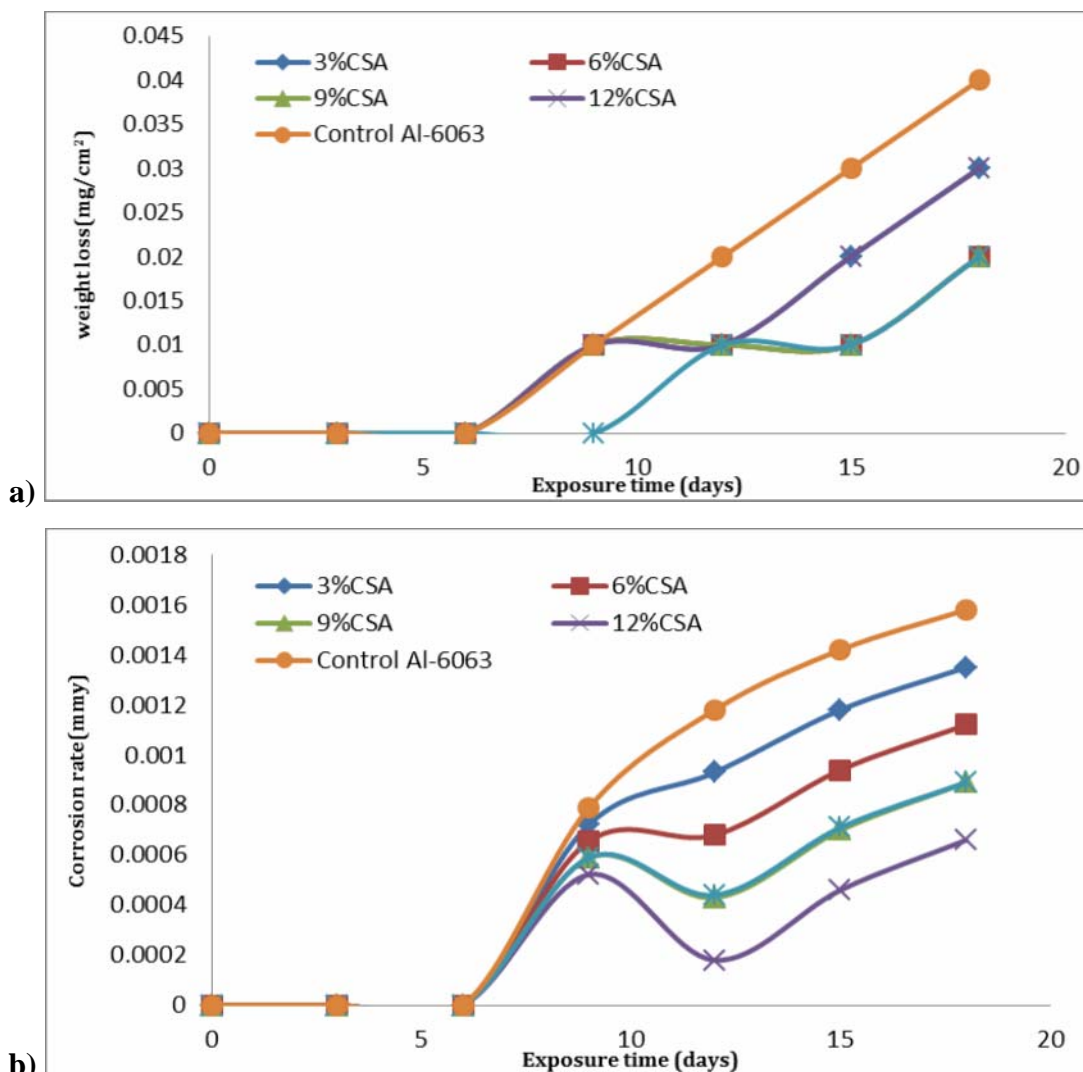


**Figure 10 (a) and (b).** Variation of (a) weight loss and (b) corrosion rate with exposure time for the CSAp reinforced Al-6063 composites in 3.5wt% NaCl solution

However, Figure 10a shows the variation of weight loss against exposure time of the samples with varying percent CSA. The rate of corrosion of the composites is in agreement with the trends observed in Figure 9.

From figure 10(a) and (b); the variation of mass loss and corrosion rate with exposure time for composite samples immersed in 3.5% NaCl solution is represented. It was observed that the passive film formed by the reinforcement in the composites which is stable for all composition significantly inhibited corrosion rate in the salt environment which in turn makes the composite more suitable than the un-reinforced Aluminium in salt environments.



## Conclusions

From the results and discussion above the following conclusions can be made:

1. Aluminum alloy/coconut shell ash composites were synthesized successfully by using stir casting technique. The density decreases as the percentage of coconut shell increases in the alloy. An indicator that composites of lower weight component can be produced.
2. The microstructural examination shows the sparcely distribution of coconut shell ash particles in the Aluminium alloy matrix. The interfacial bonding between the alloy and the coconut shell ash particles resulted in the lower values of pore in the composites.
3. Incorporation of coconut shell particles in Aluminium matrix can lead to the production of low cost Aluminium composites with improved hardness values and tensile strength.
4. In 3.5wt% NaCl solution, it was observed that the resistance to corrosion decreases with increase in percentage of coconut shell ash particles with the composite having 12wt% CSA exhibiting the best resistance to corrosion. In 3.0M H<sub>2</sub>SO<sub>4</sub> solution, the composites were generally a bit more susceptible to corrosion compared to 3.5% NaCl solution.

## References

1. Christy T. V., Murugan N., Kumar S., *Comparative study on the microstructures and mechanical properties of Al 6061 alloy and the MMC Al 6061/TiB2/12p*. Journal of Minerals and Materials Characterization and Engineering, 2010, 9, p. 57-65.
2. Rohatgi P., Schultz B., *Light weight metal matrix composites-stretching the boundaries of metals. Material*, Matters, 2007, 2, p. 16-9.
3. Prasad D. S., Shoba C., Ramanaiah N., *Investigations on mechanical properties of Al hybrid composites*, Journal of Material Research and Technology, 2014, 3(1), p. 79-85.
4. Madakson P. B., Yawas D. S., Apasi A., *Characterization of coconut shell ash for potential utilization in metal matrix composites for automotive applications*, International Journal of Engineering Science and Technology, 2012, 4(3), p. 1190-1198.
5. Olugbenga O. A., Akinwole A. A., *Characteristics of bamboo leaf ash stabilization on lateritic soil in highway construction*. International Journal of Engineering and

Technology, 2010, 2, p. 212-219.

6. Prasad S. D., Krishna R. A., *Tribological properties of A356.21RHA composites*. Journal of Material Science and Technology, 2012, 28, p. 367-372.
7. Zuhailawati H., Samayamuthirian P., Mohd Haizu C. H., *Fabrication of low cost aluminum matrix composite reinforced with silica sand*. Journal of Physical Science, 2007, 18, p. 47-55.
8. Valdez S., Campillo B., Perez. R., Martinez L., Garcia H., *Synthesis and microstructural characterization of Al-Mg alloy-SiC particulate composite*, Materials Letters, 2008, 62(17-18), p. 2623-2625.
9. Apasi A., Madakson P. B., Yawas D. S., Aigbodion V. S., *Wear behaviour of Al-Si-Fe alloy/coconut shell ash particulate composites*, Tribology in Industry, 2012, 34(1), p. 36-43.
10. Alaneme K. K., Olubambi P. A., Afolabi A. S., Bodunrin M. O., *Corrosion and Tribological Studies of Bamboo Leaf Ash and Alumina Reinforced Al-Mg-Si alloy matrix hybrid composite in chloride medium*, Int J Electrochem Sci., 2014, 9, p. 5663-5674.
11. Aleneme K. K., Eze H. I., Bodunrin M. O., *Corrosion behaviour of groundnut shell ash and silicon carbide hybrid reinforced Al-Mg-Si alloy composites in 3.5% NaCl and 0.3M H<sub>2</sub>SO<sub>4</sub>*, Leonardo Electronic Journal of Practices and Technologies, 2015, 26, p. 129-146.
12. Alaneme K. K., *Influence of Thermo-mechanical Treatment on the Tensile Behaviour and CNT evaluated Fracture Toughness of Borax premixed SiCp reinforced Aluminium (6063) Composites*, International Journal of Mechanical and Materials Engineering, 2012, 7(1), p. 96-100.
13. ASTM E 8M. *Standard Test Method for Tension Testing of Metallic Materials (Metric)*, Annual Book of ASTM Standards, Philadelphia, 1991.
14. Alaneme K. K., Bodunrin M. O., *Corrosion behaviour of alumina reinforced Al (6063) metal matrix composites*, Journal of Minerals and Materials Characterisation and Engineering, 2011, 10(2), p. 1153-1156.
15. ASTM G31. *Standards Metals Test Methods and Analytical Procedures*, Wear and Erosion; 3, Metal Corrosion, Annual Book of ASTM Standards, Philadelphia, 1994.
16. Alaneme K. K., Ademilua B. O., Bodunrin M. O., *Mechanical Properties and Corrosion*



*Behaviour of Aluminium Hybrid Composites Reinforced with Silicon Carbide and Bamboo Leaf Ash*, Tribology in Industry, 2013, 35(1), p. 25-35.

17. Agunsoye J. O., Talabi S. I., Bello S. A., Awe I.O., *The effects of cocos Nucifera (coconut shell) on the mechanical and Tribological properties of recycled waste Aluminium can composites*. Tribology in Industry, 2014, 36(2), p. 155-162.